Computational Study of Iron(II) Systems Containing Ligands with Nitrogen Heterocyclic Groups

R. A. Kirgan and D. P. Rillema*

Department of Chemistry, Wichita State University, 1854 North Fairmount, Wichita, Kansas 67260

Received: August 7, 2007; In Final Form: September 20, 2007

Density functional theory (DFT) calculations show the higher energy HOMO (highest occupied molecular orbital) orbitals of four iron(II) diimine complexes are metal centered and the lower energy LUMO (lowest unoccupied molecular orbitals) are ligand centered. The energy of the orbitals correlates with electrochemical redox potentials of the complexes. Time-dependent density functional theory (TDDFT) calculations reveal ligand centered (LC) and metal-to-ligand charge transfer (MLCT) at higher energy than experimentally observed. TDDFT calculations also reveal the presence of d−d transitions which are buried under the MLCT and LC transitions. The difference in chemical and photophysical behavior of the iron complexes compared to that of their ruthenium analogues is also addressed.

Introduction

Iron(II) diimine complexes show similar electronic and chemical properties.[1−8] Compared to its congener, ruthenium(II) which has the same d^6 electronic configuration, the iron(II) analogues are less stable and undergo ligand loss more readily. When diimine ligands, such as bipyridine, are bound to ruthenium the molecule is very stable under most conditions, but when bound to iron, a decomposition reaction occurs, which is thought to be thermally and photochemically driven. Ligand loss occurs very rapidly in some cases such as in $Fe(bpz)_3^{2+}$. In others, such as in $Fe(bpy)_3^{2+}$, it occurs more slowly.

In an attempt to understand the variation in the properties between iron(II) and ruthenium(II) and the differences in stability between iron(II) diimine complexes, we report a general computational study on four iron(II) complexes used to ascertain these differences. We[8,9] and others[10,11] have examined ruthenium(II) complexes in the past; here we focus on three iron(II) diimine systems, 2,2′-bipyridine, 2,2′-bipyrazine, and 1,10-phenanthroline,[13−24] and one iron (II) triimine, $Fe(terpy)_2^{2+}$, where terpy is 2,2′:6′,2″-terpyridine, shown in Figure 1.

Computational Technique

The geometries of the complexes **1**−**4** (Figure 1) were optimized in the singlet ground state without symmetry constraints in the gas phase using the B3LYP[25] functional of the Gaussian '03 program package.[26] The Stuttgart-Dresden (SDD)[27] ECP was utilized for all the atoms in the molecule. The specific effective core potential-basis set used for iron was the Stuttgart-Dresden-double-ζ basis set (6d, 10f), and the D95V basis set was used for all other atoms.

TDDFT[28] calculations were employed to produce a number of singlet excited states of the complex ions based on their singlet ground-state optimized geometry in the gas phase. The number of singlet−singlet transitions calculated for complex **1** was 50; complex **2**, 100; complex **3**, 75; and complex **4**, 50. The output contained information for the excited-state energies, oscillator strengths (*f*), and a list of the transitions that give rise to each excited state. The orbitals involved as well as the orbital contribution coefficients of the transitions were obtained. All transitions with $f > 0.0000$ were considered to search for the possibility of d−d transitions. GaussSum[29] was used to generate both simulated spectra and orbital information. The molar absorptivity was calculated with a full-width-at-half-maximum of 3000 cm^{-1}.

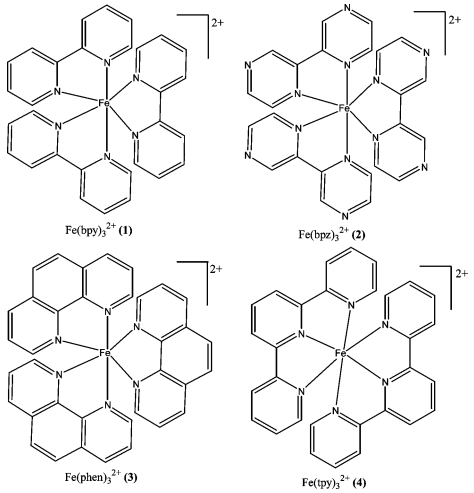

Figure 1. Schematic drawing of complexes **1**−**4**.

Geometry Optimization. All optimized calculated structures have been compared to crystal structures. The bond distances between the Fe atoms and the nitrogen atoms are listed in Table 1. All of the crystals used for comparison had the same counterion as to avoid any anomalies in the packing. The average difference for all the bond lengths was 0.042 ± 0.012 Å (24 values) longer than the experimental values. The B3LYP/6-311G(d) and UB3LYP/6-311G(d,p) basis sets were compared for complex **2** but no appreciable difference was found, so the B3LYP/SDD basis set was used for all calculations.

The structures of all the complexes contain two shorter axial bound nitrogen atoms than the ones in the equatorial position. The calculations mimic this effect but with very little change between the axial and equatorial distances. These complexes

* Author to whom correspondence should be addressed. E-mail: paul.rillema@wichita.edu.

10.1021/jp076334t CCC: $37.00
Published on Web 11/28/2007

TABLE 1: Experimental vs Calculated Bond Distances

	1		2		3		4	
	expt[30]	calcd	expt[1]	calcd	expt[31]	calcd	expt[32]	calcd
Fe−N	1.947	2.009	1.953	2.007	1.966	2.017	1.890	1.913
Fe−N	1.949	2.009	1.957	2.007	1.973	2.018	1.891	1.913
Fe−N	1.953	2.010	1.961	2.008	1.980	2.018	1.978	2.019
Fe−N	1.961	2.010	1.966	2.008	1.981	2.019	1.984	2.019
Fe−N	1.964	2.010	1.966	2.008	1.984	2.019	1.988	2.020
Fe−N	1.964	2.010	1.967	2.008	1.984	2.019	2.001	2.020
average	1.956	2.010	1.962	2.008	1.978	2.018	1.955	1.984
average diff.	0.054		0.046		0.040		0.029	

TABLE 2: Detailed HOMO, LUMO, LUMO+1, and LUMO+2 Electron Density Distribution[a]

	HOMO				LUMO			
compd	%M	%L	%L	%L	%M	%L	%L	%L
1	88	4	4	4	4	1	54	41
2	87	4	5	4	5	2	53	40
3	86	4	5	5	4	4	52	40
4	78	11	11		4	15	81	
$Ru(bpy)_3^{2+}$	82	6	6	6	1	33	33	33
$Ru(bpz)_3^{2+}$	82	6	6	6	1	33	33	33

	LUMO+1				LUMO+2			
compd	%M	%L	%L	%L	%M	%L	%L	%L
1	4	12	23	61	0	35	34	31
2	5	10	24	61	0	34	33	33
3	4	12	24	60	0	34	32	34
4	4	15	81		0	51	49	
$Ru(bpy)_3^{2+}$	6	7	27	60	6	3	36	55
$Ru(bpz)_3^{2+}$	8	12	19	61	8	1	42	50

[a] Ligands are arbitrary, the percentages are organized by increasing number.

are like most *tris* chelated metal complexes which have a D_3, "propeller" geometry.

Molecular Orbitals. The molecular orbital diagrams in Figure 2 show the electron density distribution in the HOMO and LUMO orbitals. The data for the composition of the HOMO, LUMO, LUMO+,1 and LUMO+2 are listed in Table 2. For the compounds **1**−**3**, ∼87% of the electron density in the HOMO is located on the metal and 4% is distributed on each of the three ligands. Compound **4** has less electron density located on the metal (78%) and 11% located on each of the two ligands.

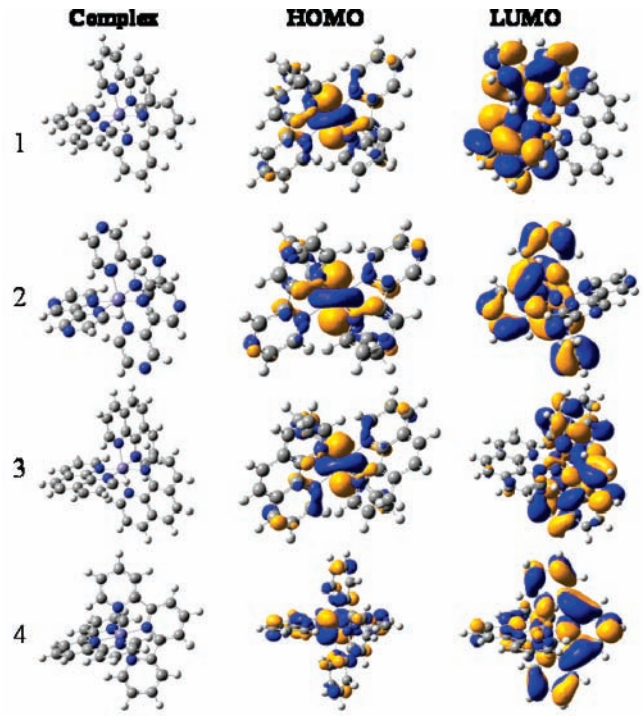

Figure 2. Molecular orbital diagrams for the optimized structure and HOMO and LUMO orbitals.

As shown in Figure 2, the LUMO is primarily localized on the ligands, but not symmetrically as found for ruthenium(II) analogues.[33] For compounds **1**−**3**, ∼53% lies on one ligand and ∼40% on another, and the remaining is distributed on the metal and the third ligand. For compound **4**, 81% is localized on one ligand, 15% on the other, and 4% on the metal. The LUMO+1 for compounds **1**−**3** follows a similar pattern as in the LUMO. In this case, ∼61% is localized on one ligand, ∼24% on another, and the remainder on the third ligand and the metal. The distribution in the LUMO+1 for compound **4** is the same as the LUMO. Only the LUMO+2 is evenly localized among the ligands with no localization on the iron atom.

Orbital Energy Levels. Figure 3 shows the energies of the 12 frontier orbitals for each of the complexes. The complexes show a similar orbital distribution within the occupied and virtual orbital energy levels. In all cases the HOMO, HOMO-1, and HOMO-2 orbital energies are iron centered; all of the other orbital energies are ligand centered. The complexes have similar energy gaps, but the HOMO and LUMO orbitals of $Fe(bpz)_3^{2+}$ are lower in energy than those of the others.

The energies of the orbitals for complexes **1**, **3**, and **4** are similar since the ligands have similar π structures. The LUMO orbitals of the phenanthroline ring are slightly higher in energy but their spacing is much smaller than for the bipyridine ring. Similarly, the energy level of the HOMO orbital of phenanthroline complex is higher than that of the bipyridine analogue. In the terpyridine system, both the HOMO and LUMO orbitals are lower in energy then in the bipyridine complex; the LUMO

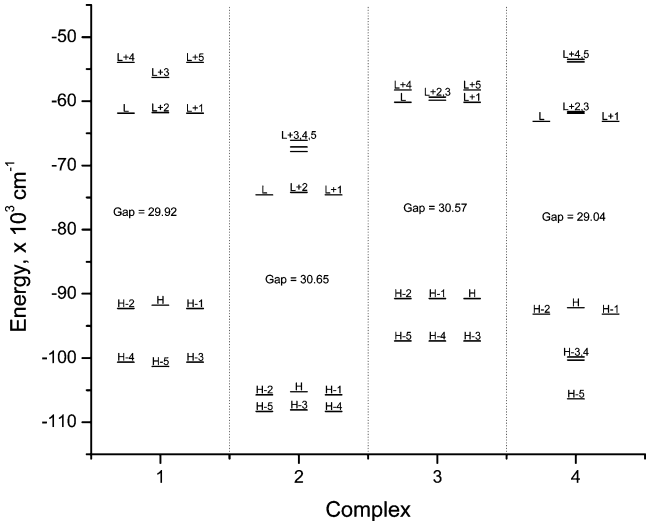

Figure 3. Six occupied and six virtual frontier orbitals.

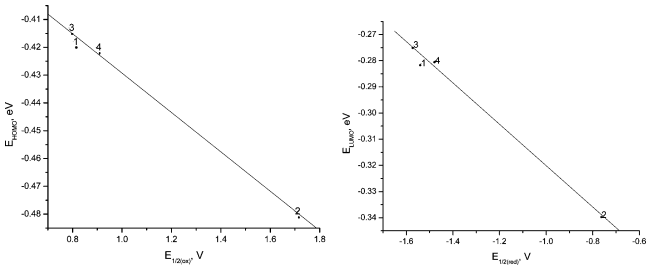

Figure 4. Left*:* Plot of HOMO energy vs oxidation potential. Right*:* Plot of LUMO energy vs first reduction potential. 1: $Fe(bpy)_3^{2+}$; 2: $Fe(bpz)_3^{2+}$; 3: $Fe(phen)_3^{2+}$; 4: $Fe(tpy)_2^{2+}$.

TABLE 3: Electrochemical Data and Mulliken Charges

	oxidation	reductions			
complex	$E_{1/2}$	$E_{1/2}(1)$	$E_{1/2}(2)$	$E_{1/2}(3)$	MC[a]
1[b]	0.80	−1.54	−1.72	−1.90	1.016
2	1.70	−0.76	−0.92	−1.20	1.073
3[b]	0.79	−1.57	−1.76	−1.85	1.014
4[b]	0.90	−1.48	−1.66		1.107
$Ru(bpy)_3^{2+}$ [c]	1.27	−1.31	−1.50	−1.77	1.117
$Ru(bpz)_3^{2+}$ [c]	1.98	−0.68	−0.87	−1.14	1.233

[a] Mulliken charge on iron center. [b] Reference 2. [c] Reference 26.

orbital energies have a greater decrease in energy than the HOMO orbitals.

Discussion

Electrochemical Behavior. Electrochemical data and Mulliken charges obtained from the computational studies are listed in Table 3. Complexes **1**−**3** have three reversible reductions and one reversible oxidation; complex **4** has only two reversible reductions and one reversible oxidation as reported.[3] Linear correlations between the first reduction potential and the energy of the LUMO for a series of ruthenium(II) diimine complexes have been reported in the past.[33] Here the energy of the LUMO also correlates with the first reduction potential of the iron(II) complexes with a slope of -0.399 ± 0.006 ($R^2 = 1.00 \pm 0.01$) as shown in Figure 4. Similarly, the energy of the HOMO for the four complexes also correlates with their oxidation potentials. The graph in Figure 4 is linear with a slope of -0.358 ± 0.004 ($R^2 = 1.00 \pm 0.01$). While the plots are linear, additional points at intermediate potentials would be desirable to substantiate the observed trends.

Energy Levels. The electrochemical potential trends indicate electron density changes occur in the molecular orbitals of the complexes altering their energy levels. The most difficult complex to oxidize and easiest to reduce, complex **2**, has the lowest energy HOMO and LUMO, as well as the highest Mulliken charge. This is consistent with the greater electron withdrawal power of the bipyrazine ligand rendering the iron(II) center more positive than the other two. In like manner, the slightly less positive charge on the iron(II) center for the phenanthroline derivative compared to that of the bipyridine analogue is consistent with less electron density being withdrawn from the iron(II) center when phenanthroline is coordinated. The iron(II) terpyridine complex has a high Mulliken charge and clearly does not follow the rationale discussed for the other three complexes. This is due to geometry factors related to the tridentate-terpyridine ligand.

The splitting and spacing patterns of the LUMO orbitals is different for complex **1** and **3**. The pattern of the first three orbitals (L, L+1, L+2) is similar, but the next three have a much larger spacing. The energy gap from the orbitals labeled L+2 to L+3 increases in energy from complex **3** to **1.** This is most likely related to the greater aromaticity of the phenanthroline ligand.

Singlet Excited States and UV−Vis Absorption Spectra. The singlet excited-state spectra were calculated and are displayed in Figure 5; the calculated and experimental transition energies along with assignments are tabulated in Table 4. The electronic transitions corresponding to excitation from one electronic level to another are composed of several, often commensurable, orbital-to-orbital transitions represented by the vertical lines underneath the spectral envelopes. A complete list of the assignments can be found in the Supporting Information (S1−4).

Iron(II) differs from most other metal complexes studied using DFT and TDDFT calculations. First, it is a 3d transition element ,and so d−d transitions are expected due to low-lying d orbitals. Second, the complexes have residual paramagnetism. For example, complex **1** has a magnetic moment of ∼1 μ_B;[34] complex **2** has one of 0.7 μ_B.[1]

Electronic d−d transitions have low absorption coefficients; therefore in the calculated spectra these would have low oscillator strengths. Examination of the time-dependent density functional theory data related to d−d transitions is tabulated in Table 5. There are d−d transitions scattered throughout the spectra and buried under more intense transitions. Each complex has about two or three d−d transitions located at lower energy than the metal-to-ligand charge transfer bands. They are not pure d−d transitions, but a good percentage of the transition is d−d, generally greater than 80%. The calculated extinction coefficients of these transitions are very small to moderate (∼50 to ∼300 M^{-1} cm^{-1}), as would be expected.

Generally for each complex the $\pi \rightarrow \pi^*$ transitions occur at high energy (30 000−45 000 cm^{-1}) and are ligand centered (LC). The peak ∼ 24 000 cm^{-1} is assigned as mostly metal-to-ligand charge transfer (MLCT). The calculated absorption maxima are blue-shifted from the experimental maxima ∼3000 cm^{-1} for the LC transitions and ∼4000−5000 cm^{-1} for the MLCT transitions. Each of the basis sets mentioned in the geometry optimization section were tried to find a solution to this, but they all gave similar results. While this red shift has often been found for other metal complexes and corrected by incorporating solvent into the calculation,[12,13,36] in these systems only small red shifts were found when solvent is introduced into the calculations. A method used to correct the calculated energy maxima using a correlation between experimental MLCT maxima and calculated maxima as previously reported[37] was

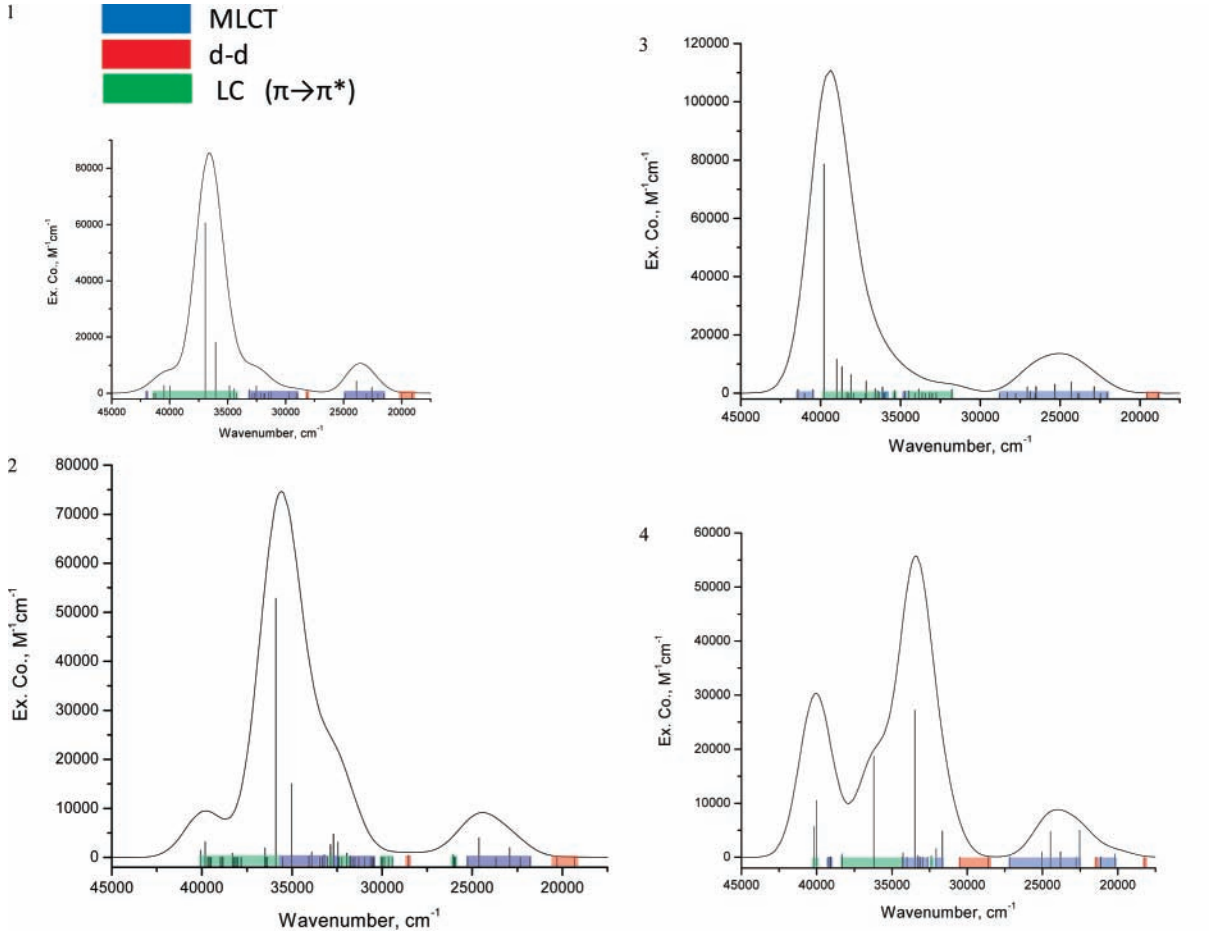

Figure 5. Singlet excited-state spectra with transitions shown as vertical bars.

TABLE 4: Tabulated Data for the Experimental and Calculated Spectra

complex	E_{exp} (ϵ, M^{-1} cm^{-1})[a]	E_{calc}[b]	assignment
1	32.9 (58 000)	36.7	$\pi \rightarrow \pi^*$
	19.2 (11 200)	23.6	MLCT
2	32.7 (55 000)	35.6	$\pi \rightarrow \pi^*$
	18.2 (12 300)	24.4	MLCT
3	23.0 (7 300)	26.5	MLCT
	19.4 (11 200)	24.8	MLCT
4	36.5 (40 500)	40.0	$\pi \rightarrow \pi^*$
	31.4 (38 000)	33.4	$\pi \rightarrow \pi^*$
	17.8 (12 000)	24.0	MLCT

[a] In DMF. [b] In gas phase.

TABLE 5: Calculated d−d Transitions and Absorption Coefficients

	1	2	3	4	$Ru(bpy)_3^{2+}$	$Ru(bpz)_3^{2+}$
energy	19089	19322	18856	21424		
ex. co.[a]	46.3	46.3	15.4	23.1		
energy	19097	19328	18864	21436		
ex. co.[a]	46.3	46.3	23.1	23.1		
energy	28142	28533	28309	28583	31728	32091
ex. co.[a]	239.2	362.7	185.2	0	547.8	208.3
energy	28149	28540	28315	28607	31738	32109
ex. co.[a]	246.9	362.7	185.2	0	509.3	177.5

[a] Reference 35, using a FWMH of 3000 cm^{-1}.

also unsuccessful. There was no correlation found with the MLCT transitions.

The inability to mimic experimental spectra more closely may be due to residual paramagnetism of the complex. This is quite large for a low-spin "diamagnetic" iron center, but there are many other examples of this phenomenon.[34] To investigate this further and allow for the spin anisotropy, the unrestricted UB3LYP/6-311g(d,p) basis set was chosen. Yet again all three of the basis sets, B3LYP/6-311G(d), UB3LYP/6-311G(d,p), and B3LYP/SDD, yielded an S^2 value of 0.000 for all complexes.

The experimental transitions are located on a Tanabe-Sugano diagram approximately near the spin crossover line. The calculated transitions reside well within the low-spin region of the diagram. Thus, the theory or basis sets appear, at this time, unable to effectively treat data, although a multiconfigurational approach, such as CASSCF/CASPT2, may be appropriate but is out of the scope of this paper. These compounds are being investigated using Mossbaüer and EPR spectroscopy to determine if the residual paramagnetism effect observed comes from the iron center or the molecule as a whole. The results will be discussed in a later paper along with any new calculations that might result.

Comparison to Ru(II). Ruthenium tris-2,2′-bipyridine has been treated by computational methods similar to those described for the iron complexes, and the results presented are of the present work. The HOMO orbital for all four iron complexes and the ruthenium complex shows that ∼85% of the electron density resides on the metal center; the other 15% is distributed equally among the ligands. On the other hand the LUMO orbital of $Ru(bpy)_3^{2+}$ is symmetrically localized on the ligands unlike the iron complexes where it is unequally distributed. For complexes **1**−**3**, ∼90% of LUMO orbital is localized on two ligands and the remaining ligand has less than 5%. For complex **4** the LUMO localization for one terpyridine ring has 81% and the other has only 15%. The LUMO+1 orbital is unequally localized for both the iron and ruthenium complexes. The opposite result of the LUMO orbital is found for the LUMO+2

orbital. The iron complexes have an equal distribution whereas the ruthenium complexes have an unequal distribution. The reason for these localized effects may be related to π back-bonding differences in the Fe(II) and Ru(II) diimine complexes. The first reduction potential for $Fe(bpy)_3^{2+}$ is located at -1.54 V, but for $Ru(bpy)_3^{2+}$ it is found at -1.31 V. The oxidation potentials are 0.80 and 1.27 V, respectively. These more positive shifts for Ru(II) represent greater π back-bonding in its case than for Fe(II) which may account for the unequal localization of the LUMO on the ligands.

In the iron complexes the LUMO and LUMO+1orbitals are degenerate, and the LUMO+2 orbitals are 0.01, 0.05, 0.04, and 0.16 eV higher in energy for compounds **1**−**4**, respectively. The LUMO+1 and +2 are higher in energy than the LUMO by 0.13 and 0.16 eV for $Ru(bpy)_3^{2+}$ and $Ru(bpz)_3^{2+}$, respectively. The energy of the LUMO for $Ru(bpy)_3^{2+}$ is 0.082 eV higher than for $Fe(bpy)_3^{2+}$.

The energy of the HOMO orbitals is dependent on their Mulliken charges. For $Ru(bpy)_3^{2+}$ the Mulliken charge is more positive than for $Fe(bpy)_3^{2+}$, hence its HOMO is lower in energy.

Chemical Behavior. Iron complexes have been known for many years to undergo rather rapid ligand substitution reactions and to have a very strong attraction to certain anions such as chloride, bromide, and thiocyanate, which have all been shown to cause thermal dissociation reactions.[38−50] Such reactions are accelerated in the presence of light. Ruthenium complexes, on the other hand, are stable under most conditions but do undergo slow photosubstitution in the presence of excess halide.[51] Lability of transition metal complexes has long been attributed to paramagnetism and to population of dσ* states which perturb the bonding interaction. The thermal reaction of iron complexes in the dark is attributed to residual paramagnetism.

The d−d transitions in the iron complexes found by TDDFT calculations would allow light to populate the dσ* states rendering the complexes labile. The TDDFT calculation in the case of $Ru(bpy)_3^{2+}$ does not result in predicted d−d transitions at similarly low energy as found in the iron complexes. Hence, the ruthenium(II) diimine complexes are more stable to photosubstitution reactions. Ruthenium(II) complexes also do not have residual paramagnetism; hence, they are much more thermally stable than their iron(II) analogues.

Conclusions

A general computational study has been completed on four different but similar iron(II) diimine complexes. This paper brings to light the difference in the molecular orbital behavior but shows how the complexes overall behave as other diimine metal complexes. We hope this investigation will encourage others to begin an in-depth investigation into a theoretical basis for treating systems with residual paramagnetism.

Acknowledgment. We are grateful for the support from the Graduate Assistance in Areas of National Need, State of Kansas; the Wichita State University High Performance Computing Center; the Wichita State University Office of Research Administration; and the Department of Energy.

Supporting Information Available: The optimized geometries, the percent orbital contributions, and the calculated singlet excited-state energies of the four complexes. This material is available free of charge via the Internet at http://pubs.acs.org.

References and Notes

(1) Toma, L. M.; Eller, C.; Rillema, D. P.; Ruiz-Pérez, C.; Julve, M. *Inorg. Chim. Acta* **2004**, *357*, 2609.
(2) Gillard, R. D.; Knight, D. W.; Williams, P. A. *Transition Met. Chem* **1979**, *4*, 375.
(3) Braterman, P. S.; Song, J.-I.; Peacock, R. D. *Inorg. Chem.* **1992**, *31*, 555.
(4) Ruminski, R. R.; Van Tassel, K. D.; Peterson, J. D. *Inorg. Chem.* **1984**, *23*, 4380.
(5) Constable, E. C.; Ward, M. D.; Corr, S. *Inorg. Chim. Acta* **1988**, *141*, 201.
(6) Krumholz, P. *Inorg. Chem.* **1965**, *4*, 612.
(7) Palmer, R. A.; Piper, T. S. *Inorg. Chem.* **1966**, *5*, 864.
(8) Song, J.-I. Ph.D. Thesis, University of Glasgow, Scotland, 1989.
(9) Stoyanov, S. R.; Villegas, J. M.; Rillema, D. P. *Inorg. Chem. Commun.* **2004**, *7*, 838.
(10) Villegas, J. M.; Stoyanov, S. R.; Huang, W.; Lockyear, L. L.; Reibenspies, J. H.; Rillema, D. P. *Inorg. Chem.* **2004**, *43*, 6383.
(11) Fantacci, S.; De Angelis, F.; Sgamellotti, A.; Re, N. *Chem. Phys. Lett.* **2004**, *396*, 43.
(12) Vlcek, A., Jr; Zalis, S. *J. Phys. Chem. A* **2005**, *109*, 2991.
(13) Neumann, H. M.; Van Meter, F. M. *J. Am. Chem. Soc.* **1976**, *98*, 1382.
(14) Ortega, F.; Rodenas, E. *J. Phys. Chem.* **1986**, *90*, 2408.
(15) Lee, T. S.; Kolthoff, I. M.; Leussing, D. L. *J. Am. Chem. Soc.* **1948**, *70*, 3596.
(16) Blandamer, M. J.; Burgess, J.; Fawcett, J.; Guardado, P.; Hubbard, C. D.; Nuttall, S.; Prouse, L. J. S.; Radulovi_, Russell, D. R. *Inorg. Chem.* **1992**, *31*, 1383.
(17) Lawrance, G. A.; Stranks, D. R.; Suvachittanont, S. *Inorg. Chem.* **1979**, *18*, 82.
(18) Blandamer, M. J.; Burgess, J. *Pure Appl. Chem.* **1982**, *54*, 2285.
(19) Dickens, J. E.; Basolo, F.; Neumann, H. M. *J. Am. Chem. Soc.* **1957**, *79*, 1286.
(20) Ortega, F.; Rodenas, E. *Can. J. Chem.* **1989**, *67*, 305.
(21) Blanamer, M. J.; Burgess, J.; Clark, B. *J. Chem. Soc., Chem. Commun.* **1983**, 660.
(22) Burgess, J.; Prince, R. H. *J. Chem. Soc.* **1965**, 4697.
(23) Margerum, D. W.; Morgenthaler, L. P. *J. Am. Chem. Soc.* **1962**, *84*, 706.
(24) Blandamer, M. J.; Burgess, J. *Pure Appl. Chem.* **1983**, *55*, 55.
(25) (a) Becke, A. D. *J. Chem. Phys.* **1993**, *98*, 5648. (b) Lee, C.; Yang, W.; Parr, R. G. *Phys. Rev. B* **1988**, *37*, 785. (c) Vosko, S. H.; Wilk, L.; Nusair, M. *Can. J. Phys.* **1980**, *58*, 1200.
(26) Frisch, M. J.; Trucks, G. W.; Schlegel, H. B.; Scuseria, G. E.; Robb, M. A.; Cheeseman, J. R.; Montgomery, J. A., Jr.; Vreven, T.; Kudin, K. N.; Burant, J. C.; Millam, J. M.; Iyengar, S. S.; Tomasi, J.; Barone, V.; Mennucci, B.; Cossi, M.; Scalmani, G.; Rega, N.; Petersson, G. A.; Nakatsuji, H.; Hada, M.; Ehara, M.; Toyota, K.; Fukuda, R.; Hasegawa, J.; Ishida, M.; Nakajima, T.; Honda, Y.; Kitao, O.; Nakai, H.; Klene, M.; Li, X.; Knox, J. E.; Hratchian, H. P.; Cross, J. B.; Bakken, V.; Adamo, C.; Jaramillo, J.; Gomperts, R.; Stratmann, R. E.; Yazyev, O.; Austin, A. J.; Cammi, R.; Pomelli, C.; Ochterski, J. W.; Ayala, P. Y.; Morokuma, K.; Voth, G. A.; Salvador, P.; Dannenberg, J. J.; Zakrzewski, V. G.; Dapprich, S.; Daniels, A. D.; Strain, M. C.; Farkas, O.; Malick, D. K.; Rabuck, A. D.; Raghavachari, K.; Foresman, J. B.; Ortiz, J. V.; Cui, Q.; Baboul, A. G.; Clifford, S.; Cioslowski, J.; Stefanov, B. B.; Liu, G.; Liashenko, A.; Piskorz, P.; Komaromi, I.; Martin, R. L.; Fox, D. J.; Keith, T.; Al-Laham, M. A.; Peng, C. Y.; Nanayakkara, A.; Challacombe, M.; Gill, P. M. W.; Johnson, B.; Chen, W.; Wong, M. W.; Gonzalez, C.; Pople, J. A. *Gaussian 03*, Revision B.04; Gaussian, Inc.: Wallingford, CT, 2004.
(27) Andrae, D.; Hauessermann, U.; Dolg, M.; Stoll, H.; Preuss, H. *Theor. Chim. Acta* **1990**, *77*, 123.
(28) (a) Stratmann, R. E.; Scuseria, G. E.; Frisch, M. J. *J. Chem. Phys.* **1998**, *109*, 8218. (b) Bauernschmitt, R.; Ahlrichs, R. *Chem. Phys. Lett.* **1996**, *256*, 454. (c) Casida, M. E.; Jamorski, C.; Casida, K. C.; Salahub, D. R. *J. Chem. Phys.* **1998**, *108*, 4439.
(29) O'Boyle, N. M.; Vos, J. G. *Gaussum 1.0*; Dublin City University, 2005.
(30) Heilmann, J.; Lerner, H.-W.; Bolte, M. *Acta Cryst., Sect. E: Struct. Rep. Online* **2006**, *62*, m1477.
(31) Baker, J.; Engelhardt, L. M.; Figgis, B. N.; White, A. H. *J. Chem. Soc., Dalton Trans.* **1975**, 530.
(32) Baker, A. T.; Goodwin, H. A. *Aust. J. Chem.* **1985**, *38*, 207.
(33) Stoyanov, S. R.; Villegas, J. M.; Rillema, D. P. *Inorg. Chem.* **2002**, *41*, 2941.
(34) Gütlich, P. *Struct. Bonding (Berlin)* **1981**, 44 (references therein).
(35) Stoyanov, S. R.; Villegas, J. M.; Rillema, D. P. *Inorg. Chem.* **2003**, *42*, 7852.
(36) Vlček, A., Jr.; Záliš, S. *Coord. Chem. Rev.* **2007**, *251* (3−4), 258.
(37) Kirgan, R.; Simpson, M.; Moore, C.; Day, J.; Bui, L.; Tanner, C.; Rillema, D. P. *Inorg. Chem* **2007**, *46*, 6464.
(38) Neumann, H. M.; Van Meter, F. M. *J. Am. Chem. Soc.* **1976**, *98*, 1382.
(39) Ortega, F.; Rodenas, E. *J. Phys. Chem.* **1986**, *90*, 2408.

(40) Lee, T. S.; Kolthoff, I. M.; Leussing, D. L. *J. Am. Chem. Soc.* **1948**, *70*, 3596.
(41) Blandamer, M. J.; Burgess, J.; Fawcett, J.; Guardado, P.; Hubbard, C. D.; Nuttall, S.; Prouse, L. J. S.; Radulovi_, Russell, D. R. *Inorg. Chem.* **1992**, *31*, 1383.
(42) Lawrance, G. A.; Stranks, D. R.; Suvachittanont, S. *Inorg. Chem.* **1979**, *18*, 82.
(43) Blandamer, M. J.; Burgess, J. *Pure Appl. Chem.* **1982**, *54*, 2285.
(44) Dickens, J. E.; Basolo, F.; Neumann, H. M. *J. Am. Chem. Soc.* **1957**, *79*, 1286.
(45) Ortega, F.; Rodenas, E. *Can. J. Chem.* **1989**, *67*, 305.
(46) Blanamer, M. J.; Burgess, J.; Clark, B. *J. Chem. Soc., Chem. Commun.* **1983**, 660.
(47) Burgess, J.; Prince, R. H. *J. Chem. Soc.* **1965**, 4697.
(48) Margerum, D. W.; Morgenthaler, L. P. *J. Am. Chem. Soc.* **1962**, *84*, 706.
(49) Blandamer, M. J.; Burgess, J. *Pure Appl. Chem.* **1983**, *55*, 55.
(50) Kirgan, R. A.; Rillema, D. P. *Inorg. Chem.*, submitted for publication.
(51) Ross, H. B.; Boldaji, M.; Rillema, D. P.; Blanton, C. B.; White, R. P. *Inorg. Chem.* **1989**, *28*, 1013.